Annals of Nuclear Energy 128 (2019) 209–215

Contents lists available at ScienceDirect

Annals of Nuclear Energy

journal homepage: www.elsevier.com/locate/anucene

Neutronic performance characteristics of different LEU fuels in a proposed NIST research reactor

Danyal J. Turkoglu [a], Zeyun Wu [b,*], Robert E. Williams [a], Thomas H. Newton [a]

[a] NIST Center for Neutron Research, 100 Bureau Drive, Mail Stop 6101, Gaithersburg, MD 20899, USA
[b] Department of Mechanical and Nuclear Engineering, Virginia Commonwealth University, Richmond, VA 23219, USA

ARTICLE INFO

Article history:
Received 12 August 2018
Received in revised form 2 January 2019
Accepted 6 January 2019
Available online 16 January 2019

Keywords:
Low-enriched uranium
Research reactor
Neutronics performance characteristics

ABSTRACT

As a potential replacement for the National Bureau Standards Reactor (NBSR) at the U.S. National Institute of Standards and Technology (NIST), a conceptual design of a new reactor with a horizontally-split core has recently been studied using low-enriched uranium (LEU) silicide dispersion (U_3Si_2/Al) fuel. In this paper, the neutronics calculations of the proposed NIST reactor with other two low-enriched U-Mo fuels (U-10Mo monolithic fuel and U-7Mo/Al dispersion fuel) were performed, and the results were compared to that of the U_3Si_2/Al fuel, with the objective of identifying the best fuel candidate for the reactor cycle length and maximum cold neutron production. To make consistent comparisons, fuel inventories for multi-cycle equilibrium cores were produced for each fuel based on a 30 d reactor cycle at 20 MW thermal power. With its very high uranium density, the potential to load more uranium in the core with U-10Mo monolithic fuel was explored with test cases using an alternate fuel management scheme, a higher power level (30 MW), or a longer cycle (45 d). The research results indicate similar neutronics performance characteristics of the three LEU fuel options in the proposed NIST reactor with the same power level. However, the ability to load more fuel in the reactor with the U-10Mo option allows additional flexibility in the reactor design and could lead to other optimizations that maximize cold neutron production.

1. Introduction

The majority of the neutron science conducted at the National Institute of Standards and Technology (NIST) Center for Neutron Research (NCNR) utilizes cold neutrons, which are neutrons slowed down by a cold moderator to energies less than 5 meV (wavelength greater than 4 Å). Cold neutrons have been increasingly important for scientific research due to their ability to probe the structure and dynamics of soft matter in neutron scattering experiments. A conceptual design of a reactor, referred to as the NBSR-2 thereafter in this paper, is being studied as a potential replacement for the National Bureau of Standards Reactor (NBSR) (NIST, 2010), which has been operated for over 50 years at the NCNR. Feasibility studies have demonstrated the potential for the NBSR-2 design to provide bright cold neutron beams for scientific experiments (Wu and Williams, 2016; Wu et al., 2017). The proposed design, with 20 MW thermal power and a 30 d operating cycle, was selected to be on a similar scale as the NBSR. For improved neutron flux performance, the design consists of a horizontally-split compact core that is cooled and moderated by light water while reflected by heavy water (Wu et al., 2015).

The NBSR-2 employs a "tank-in-pool" design pattern, using an aluminum alloy tank (2 m height and 2 m diameter) filled with heavy water and placed in a pool of light water. Fig. 1 shows the major reactor components of the NBSR-2 in elevation and plan views. As shown in the figure, the heavy water in the tank is the reflector for the core, while the core itself is moderated and cooled by light water. The core is split horizontally to maximize the useful flux trap volume between the two halves. Each half contains nine fuel elements in a zirconium alloy box that is the boundary between light water and heavy water. Two cold neutron sources (CNSs), not yet geometrically optimized in design, are placed 25 cm from the reactor on the north and south sides of the flux trap in the heavy water tank. The positions of the CNSs balance a trade-off between cold neutron production and estimated heat load for the CNSs. Four '#' shaped hafnium alloy control blades are used for reactor control. A complete description of the NBSR-2 design can be found in Ref (Wu et al., 2017).

The fuel elements (FEs) in the design are conventional plate type for material test reactors using low-enriched uranium (LEU) with ^{235}U enrichments less than 20% mass fraction to comply with

* Corresponding author.
E-mail addresses: danyal.turkoglu@nist.gov (D.J. Turkoglu), zwu@vcu.edu (Z. Wu), robert.williams@nist.gov (R.E. Williams), thomas.newton@nist.gov (T.H. Newton).

https://doi.org/10.1016/j.anucene.2019.01.006
0306-4549/

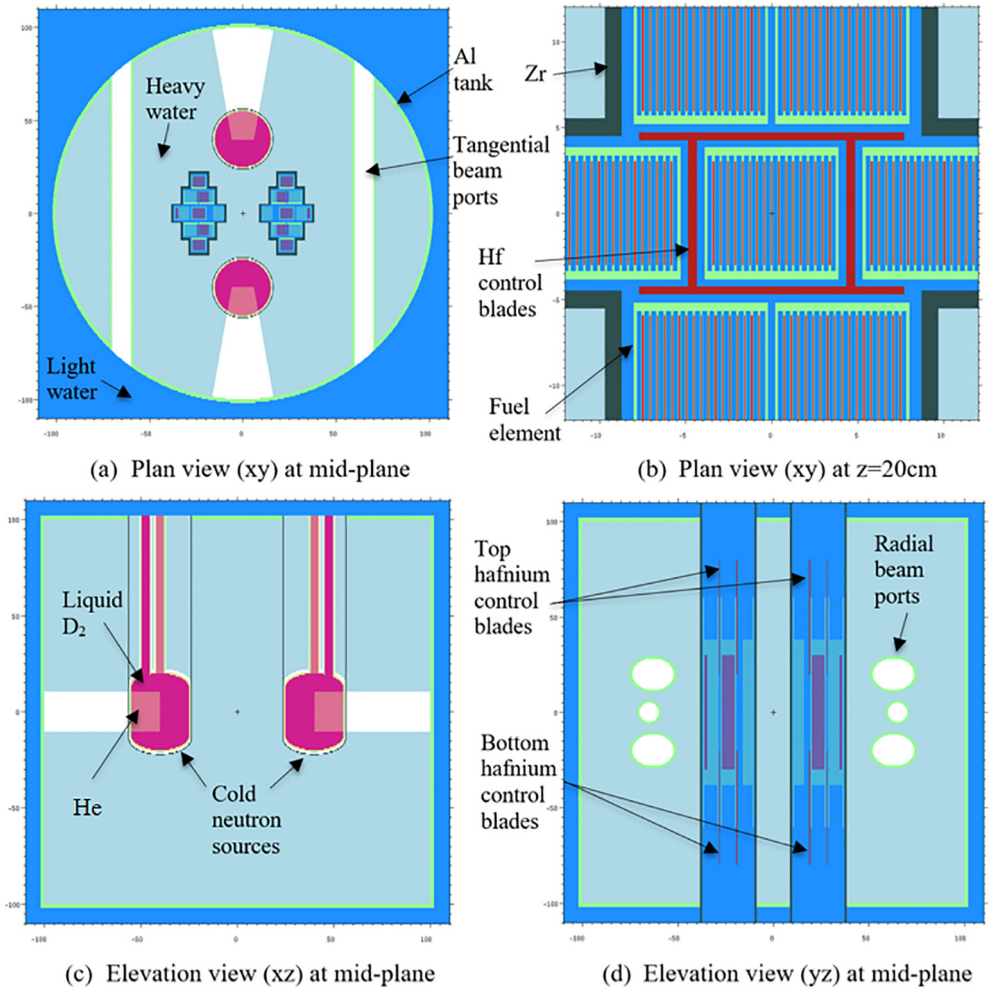

Fig. 1. Schematics representations of the NBSR-2 design. The scales have units of centimeters.

nuclear non-proliferation requirements. The U_3Si_2/Al dispersion fuel was chosen for initial studies to investigate and verify the viability of the novel design in terms of neutronics and safety performance characteristics (Wu et al., 2017). U_3Si_2/Al dispersion fuel was prioritized for the initial NBSR-2 studies because it has the highest uranium density (4.8 g/cm^3) out of the LEU fuels qualified by the US Nuclear Regulatory Commission (NRC) for use in research and test reactors (U.S. Nuclear Regulatory Commission, 1988). However, the U_3Si_2/Al dispersion fuel is not being considered as the fuel for the five high performance research reactors (HPRRs) in the United States, including the NBSR, for their conversion from high-enriched uranium (HEU) to LEU fuel. There are two reasons for seeking alternative fuels. First, low-enriched U_3Si_2/Al fuel has a relatively-low ^{235}U density, which makes it difficult to design a reactor with a very compact core (*i.e.*, high power density) due to the increased volume of fuel required. Second, the power density with U_3Si_2/Al dispersion fuel in HPRRs is also limited in the United States to comply with the current regulatory limit that the peak heat flux be less than 140 W/cm^2, which was the maximum heat flux in test elements during the fuel qualification (U.S. Nuclear Regulatory Commission, 1988). A high power density correlates to a high peak neutron flux and is, thus, a desirable attribute for the NBSR-2 design. LEU fuels containing high-density uranium molybdenum (U-Mo) alloys are being developed for use in HPRRs (Snelgrove et al., 1997) to provide similar operational and experimental performance parameters as those provided by their current HEU fuel. While the fuel conversion program in the United States is focused on U-10Mo monolithic fuel (Woolstenhulme et al., 2016), U-Mo dispersion fuels are being pursued in other countries (Leenaers et al., 2004; Ryu et al., 2013).

The primary objective of the research carried out in this paper is to investigate the neutronics performance of different LEU fuels (e.g., U-Mo fuels) in the NBSR-2 configuration. The flux performance is of the top interests to us because the main purpose of the NBSR-2 is for scientific experiments that require high flux levels; the excess reactivity and control element shut-down margin for various fuels are also of great concerns for reactor operators. In this paper, other advanced LEU fuels mentioned above, the U-Mo monolithic and dispersion fuels, were modeled in the current NBSR-2 design. The resulting neutronics performance characteristics compared with the U_3Si_2/Al dispersion fuel as a reference for their performances. A preliminary version of this study was previously presented in the recent PHYSOR meeting (Turkoglu et al., 2018). This paper includes the latest research efforts under the same work scope. It should be noted that the thermal hydraulics, safety analyses, reactor control and engineering constraints were not evaluated in this paper because these constraints are out of the scope of this study. Moreover, since the reactor studied here (*i.e*, NBSR-2) is essentially a small scale research reactor with ~20 MW thermal power, the maximum heat flux generated in the reactor is manageable with a large safety margin, as the safety analyses suggested in Ref. (Wu et al., 2017).

2. LEU fuels for high performance research reactors

The NBSR-2 was fueled in previous studies with 18 fuel elements each containing 17 plates of U_3Si_2/Al dispersion fuel. U_3Si_2/Al dispersion fuel was qualified for uranium density up to 4.8 g/cm^3 (U.S. Nuclear Regulatory Commission, 1988). Two U-Mo fuels, with higher uranium densities than U_3Si_2/Al, are considered in this work: U-7Mo/Al dispersion fuel and U-10Mo monolithic fuel, which have Mo mass fractions of 7% and 10%, respectively. The U-10Mo monolithic fuel is a pure metallic alloy that has a very high uranium density of 15.5 g/cm^3. Table 1 summarizes the chemical properties of the three LEU fuels investigated in this paper.

Reactions of U-Mo alloy with Al cladding and Al powder (in the dispersion fuel) cause the formation of interaction layers that, along with other effects such as recrystallization (Soo et al., 2013), lead to fuel swelling at high fission density values. To mitigate these adverse effects and prevent delamination in the case of U-10Mo monolithic fuel, a protective interlayer of Zr is added between the U-10Mo foil and the Al cladding (Robinson et al., 2009). The reference U-10Mo fuel system uses a 25.4 μm thick layer of Zr. Although neglected in this study, the addition of Si to the U-7Mo/Al dispersion fuel has been found to reduce the interaction layers (Leenaers et al., 2011) and mitigate fuel swelling for fission densities >3.0 × 10^{21} cm^{-3} (Hanson and Diamond, 2014).

The dimensions of the fuel meat can be adjusted to some extent by the designer of the model to achieve specific goals. For instance, the LEU fuel thicknesses were chosen to achieve similar amounts of ^{235}U in each fuel plate. The three LEU fuels were modeled with 17 plate fuel elements having a constant fuel plate thickness (0.127 cm), as shown in Fig. 2, to keep the water channel thickness constant for comparison. The parameters of the U-Mo fuels in this study are similar to those used in the preliminary analyses for the conversion of the existing NBSR from HEU to LEU (Brown and Cuadra, 2015; Hanson and Diamond, 2011).

For the U-10Mo fuel, the cladding thickness can be substantially reduced since the fuel meat is very thin, opening the possibility for 19 fuel plates in each element. The higher U loading with 19 plate fuel elements in the core presents the opportunity to: 1) extend the reactor cycle beyond 30 d, 2) extend burnup of fuel elements by burning them for more than three cycles, and/or 3) operate at higher thermal power. Thus, an MCNP6 (Pelowitz, 2012) model (code version 6.1 with ENDF/B-VII.1 data libraries) with 19 plate fuel elements was created for the U-10Mo case to explore these options. The parameters for three LEU fuels studied in this paper are summarized in Table 2. The dispersion fuels were modeled as homogeneous mixtures.

Table 1
Comparison of the three LEU fuels.

Fuel	U_3Si_2/Al	U-7Mo/Al	U-10Mo
Type	Dispersion	Dispersion	Monolithic
Compositions	U, Si, Al	U, Mo, Al	U, Mo
Enrichment (mass %)	19.75	19.75	19.75
Density (g/cm^3)	6.52	9.97	17.2
Uranium density (g/cm^3)	4.80	7.98	15.5
U-235 density (g/cm^3)	0.95	1.58	3.06

3. Research methodologies

The neutronics calculations were performed using MCNP6, a generalized Monte Carlo code for radiation transport (). Key performance characteristics of the core, such as neutron flux and fission rate, can be calculated by MCNP6 with the multi-cycle equilibrium core. To consistently obtain the fuel inventories of the multi-cycle equilibrium cores for the three LEU fuels, an iterative process was developed based on an equilibrium core search procedure (Kopetka et al., 2006). Starting from a core with all fresh fuel elements, the criticality calculation (KCODE) and depletion/burnup (BURN) features of MCNP6 were used to simulate six reactor cycles in an iterative process. Each cycle was split into four burnup states: (1) startup (SU), (2) beginning of cycle (BOC) that is 1.5 d into the cycle such that equilibrium ^{135}Xe is achieved, (2) middle of cycle (MOC) at the cycle midpoint, and (4) end of cycle (EOC).

The fuel elements (FEs) were shuffled according to one of the two fuel management schemes shown in Fig. 3. In Scheme A, the first number in the pair denotes the fuel batch number and the second number is unique identifier for the FE in the batch. In Scheme B, the first number denotes the batch number and the second number denotes the number of cycles that the element will go through. In both cases, the black and white font colors distinguish FEs in the separate cores. In Scheme A, six fresh fuel elements are added each cycle, and the six third-cycle fuel elements are discarded at the end of cycle. Scheme B uses only four fresh fuel elements each cycle, with two fourth-cycle fuel elements and two fifth-cycle elements discarded at the end of cycle. Scheme A was used for all cases except for a case with 19 plate U-10Mo fuel elements.

The fuel materials for each FE were discretized into six axial zones. To accurately model the fuel burnup in the different axial zones during the equilibrium core search process, the control blade positions were adjusted for each state using the integral worth curve and the excess reactivity of the core. Fig. 4 shows the flow diagram for the equilibrium core search process that was automated with a script for consistent application to the different cases

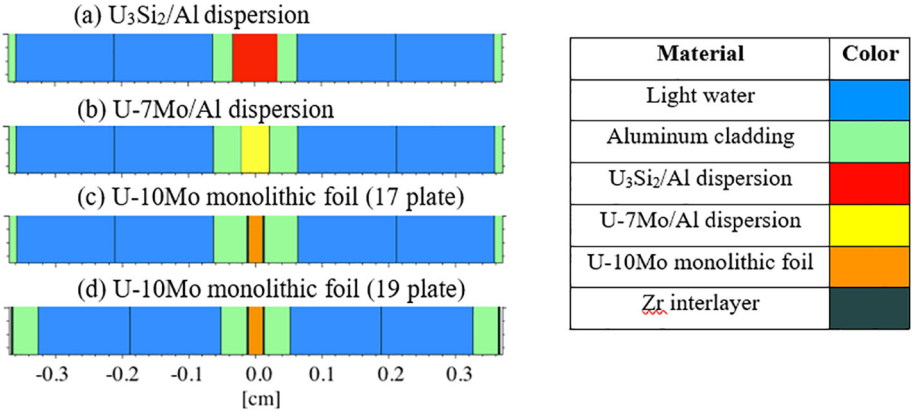

Fig. 2. The cross-sectional views of the three LEU fuels being investigated.

Table 2
Fuel parameters of the LEU Fuels.

Parameter	U_3Si_2/Al	U-7Mo/Al	U-10Mo (17[a])	U-10Mo (19[a])
Number of plates per FE	17	17	17	19
Coolant channel width (cm)	0.295	0.295	0.295	0.275
Fuel meat length (cm)	60	60	60	60
Fuel meat width (cm)	6.134	6.134	6.134	6.134
Fuel meat thickness (cm)	0.0660	0.0419	0.0216 (0.0267[b])	0.0216 (0.0267[b])
Fuel plate thickness (cm)	0.127	0.127	0.127	0.108
Cladding thickness (cm)	0.0305	0.0432	0.0502	0.0406
Fuel meat volume (cm^3)	24.31	15.14	7.95	7.95
Fuel meat mass (g)	158.48	151.22	136.83	136.83
Total U-235 mass in FE (g)	392.5	406.7	413.6	462.2

[a] The number in parenthesis refers to the number of plates in each fuel element (FE).
[b] Including the 25.4 μm Zr interlayer on both sides of the foil.

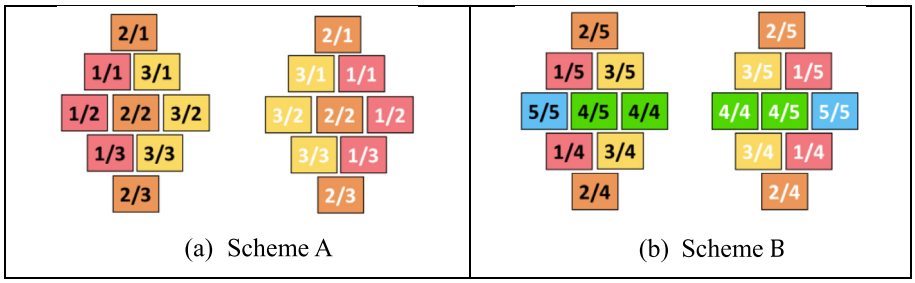

Fig. 3. The fuel management schemes used in this study.

being investigated. The process began with a core of fresh fuel elements. With the SU model of each cycle, the control blade integral worth curve was determined and subsequently used to estimate control blade positions to achieve a neutron multiplication factor, k_{eff}, of 1.01 for all states in that cycle. Following the adjustment of control blades, an updated input with the BURN card was run for the designated length to calculate the fuel depletion and fission product inventories. The fuel elements cooled down for 7 d following EOC and were reloaded based on the fuel management scheme. Six cycles were simulated for each case.

4. Results

After estimating the equilibrium core models for each LEU fuel, the fuel inventories were generated, and cold neutron source performances were compared.

4.1. Excess reactivity

Although the different LEU fuel elements contain similar amounts of ^{235}U masses in the 17 plate model, slight differences in the power distribution and neutron economy due to different neutron absorption by other materials can affect the fuel burnup, and thereby the maximum cycle length at a given power. Analyzing the results from the equilibrium core search, the excess reactivities ($\Delta\rho = \frac{k_{eff}-1}{k_{eff}}$) at each state except BOC, shown in Fig. 5(a), indicate that the LEU fuels in the 17 plate model perform similarly with a given power level, fuel management scheme and cycle length. Fig. 5(b) shows the results for excess reactivity for the 19 plate model with U-10Mo fuel using (Case 1) Scheme A with a 30 d cycle length at 30 MW, (Case 2) Scheme A with a 45 d cycle length at 20 MW and (Case 3) Scheme B with a 30 d cycle length at 20 MW. Based on these results for U-10Mo fuel, the excess

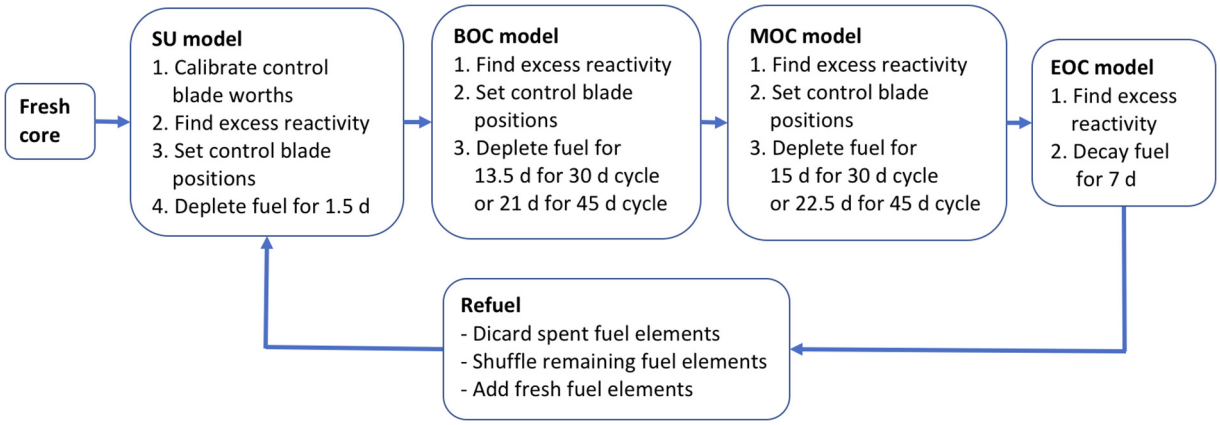

Fig. 4. The iterative process with MCNP6 for finding fuel inventories of the equilibrium core.

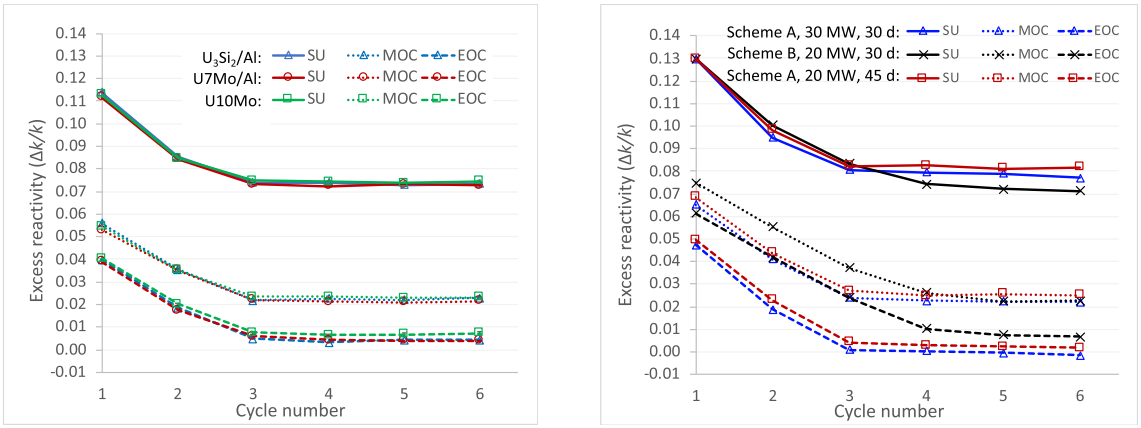

(a) 17 plate models (b) 19 plate U-10Mo model

Fig. 5. Excess reactivities at SU, MOC and EOC with control blades fully withdrawn (a) for the 17 plate models using the three LEU fuels and (b) for the 19 plate U-10Mo model.

reactivity in the 19 plate model was sufficient for 900 MW-d (MWd) of operation in Case 1 and with Scheme A of Case 2. The excess reactivity of the hybrid 4/5 batch fuel management scheme (Scheme B) in Case 3 was sufficient for 600 MWd of operation.

4.2. Fuel burnup and ^{239}Pu buildup

To examine the fuel burnup rate and additional fission contribution provided by ^{239}Pu in different fuels, Table 3 compares the fissile content of the discharged FEs after six reactor cycles for the different fuels and cycle parameters. The fissile inventories of the three LEU fuels in the 17 plate model were similar, with small differences owing to differences in the initial loadings of ^{235}U. The ^{235}U burnup for the 19 plate models of the U-10Mo fuel was significantly higher than the 17 plate models. The fissile inventories were similar despite differences in power and cycle length since each operated for 900 MWd. The results for Scheme B, with only four fresh elements at SU instead of six, had discharged elements with similar burnups to the 900 MWd cases despite only operating for 600 MWd.

4.3. Cold neutron source (CNS) performance

The primary purpose of the NBSR-2 is the production of high-intensity cold neutron beams. Cold neutrons have kinetic energies less than 5 meV and wavelengths greater than 4 Å. Intense beams of cold neutrons can be obtained from a cryogenic moderator such as liquid deuterium (LD_2) that further slows down thermal neutrons produced in the reactor. Fig. 6 illustrates a generic vertical CNS model, in which a small volume of helium offers a reentrant hole between the CNS and beam port that facilitates cold neutron transport to the guides.

One figure-of-merit measure of the CNS performance is the cold neutron surface current (in units of n/cm^{2}s) at the exit surface of the re-entrant hole as shown in the left plot in Fig. 6. The surface current of the CNS for each case was evaluated in terms of currents of cold (<5 meV), thermal (5 meV to 0.625 eV) and epithermal neutrons (>0.625 eV) at the surface of the north CNS reentrant hole. The power distribution, particularly the peaking at the center of the reactor, changes based on fuel burnup and control blade position, which can diminish the cold neutron flux by up to 10% from SU to EOC. For this evaluation, the BOC model from Cycle 6 for each case was used. The control blade inserted length was set to 10 cm for each of the four control blades. The tally results were normalized by k_{eff}, which was close to unity for each case. Additionally, the CNS heat loads were calculated with MCNP6 based on neutron, gamma-ray and beta particle heat loads in the deuterium, helium and Alumina cells; A detailed description of the heat load calculation for a CNS source can be found in Kopetka et al. (2006). Table 4 shows the results for neutron currents and heat loads.

The results in Table 4 show that the CNS performances for all cases at 20 MW were similar. Increasing the power level to 30 MW offers, not surprisingly, a 50% gain in CNS surface current – but at the expense of a proportional increase in CNS heat load to 5.4 kW. On average, the NBSR-2 design has an excellent ratio of about 6 slow neutrons per fast neutron – a metric that is important for signal-to-background ratios of scientific instruments using neutron beams. Lastly, Fig. 7 shows the flux distributions from the reactor center toward the north CNS for cold, thermal and epithermal neutrons for the 19 plate U-10Mo (45 d, Scheme A) model at BOC; These flux distributions are similar to those of the other cases at 20 MW as well as the 30 MW case except for a factor of ≈1.5 increase in values.

Table 3
Fuel burnup and ^{239}Pu mass for the discharged elements in the west core in Cycle 6.

						^{235}U burnup (%)			^{239}Pu mass (g)		
Fuel	# of fuel plates	Fuel scheme	Power (MW)	Cycle length (d)	MWd	FE 3/1	FE 3/2	FE 3/3	FE 3/1	FE 3/2	FE 3/3
U_3Si_2/Al	17	A	20	30	600	29.9	33.0	30.0	7.0	7.2	7.0
U-7Mo/Al	17	A	20	30	600	28.9	31.8	29.0	7.2	7.4	7.1
U-10Mo	17	A	20	30	600	28.2	31.2	28.4	7.2	7.5	7.3
	19	A	30	30	900	38.0	41.1	37.8	10.0	10.3	10.1
	19	A	20	45	900	37.3	40.1	37.1	9.9	10.0	9.8
						FE 4/4	**FE 5/5**		**FE 4/4**	**FE 5/5**	
	19	B	20	30	600	36.1	41.6		9.3	10.4	

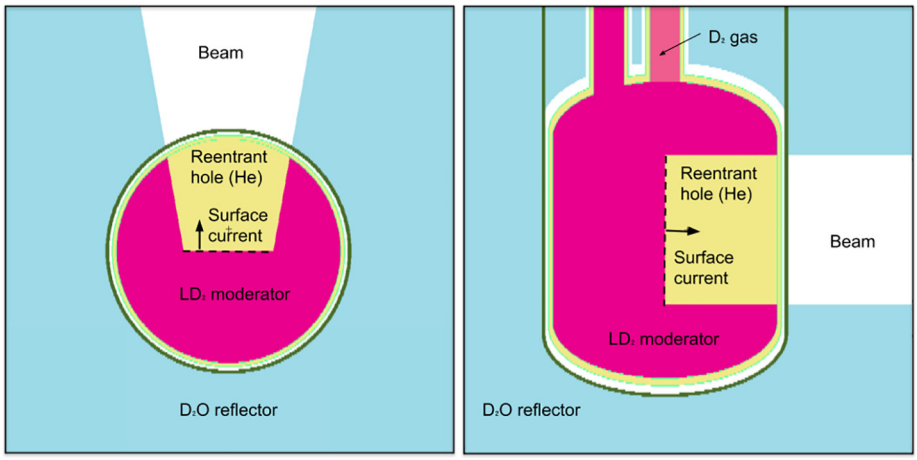

Fig. 6. A schematic top view (left) and side view (right) of the vertical CNS.

Table 4
CNS performance in terms of neutron current and heat load.

Fuel	# of fuel plates	Fuel scheme	Power (MW)	Cycle length (d)	k_{eff}	CNS current* ($\times 10^{11}$ cm^{-2})				CNS heat load (kW)
						Cold	Thermal	Epith-ermal	Total	
U_3Si_2/Al	17	A	20	30	1.000	5.4	9.8	2.2	17.5	3.7
U-7Mo/Al	17	A	20	30	0.999	5.4	9.8	2.2	17.5	3.7
U-10Mo	17	A	20	30	1.001	5.4	9.7	2.2	17.3	3.7
	19	A	30	30	1.007	7.8	14.2	3.3	25.2	5.4
	19	A	20	45	1.010	5.3	9.3	2.1	16.6	3.6
	19	B	20	30	1.000	5.3	9.7	2.2	17.3	3.7
NBSR						0.89				

* All tallies were performed with cos θ greater than 0.99, where θ is the angle between the neutron streaming direction and the normal direction of the exit surface. The relative standard errors of the tallies are all less than 0.1%.

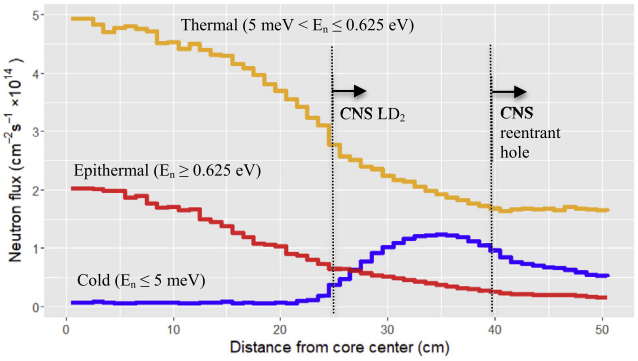

Fig. 7. The neutron flux distribution from the reactor center toward the north CNS for the 19 plate U-10Mo (45 d, Scheme A) model at BOC.

5. Summary

Three LEU fuel options – U_3Si_2/Al dispersion, monolithic U-10Mo and U-7Mo/Al dispersion – performed similarly in 17 plate FE models that kept plate thickness constant and contained similar amount mass of ^{235}U in fresh FEs. The U-10Mo model has a very thin fuel meat (0.0216 cm) that could enable more plates in a fuel element of fixed size. The neutronics analysis results reveal very similar flux performance characteristics in the NBSR-2 for the three different LEU fuels, which indicates the mass amount of ^{235}U will have a dominantly influence on the neutronics behavior in high performance reactors such as NBSR-2, if no significant variations made to external dimension and fuel cycle length of the core. However, increasing the power level to 30 MW offers, not surprisingly, will achieve a 50% gain in CNS surface current – but at the expense of a proportional increase in CNS heat load to 5.4 kW.

We also explored this possibility with a 19 plate fuel element with combinations of power levels (20 MW or 30 MW) and cycle lengths (30 d or 45 d) to demonstrate that the reactor design could potentially reach 900 MWd of operation with six fresh fuel elements per cycle. A fuel management scheme with only four fresh fuel elements, potentially lowering the operating costs, was found to be suitable for 600 MWd of operation. However, the model with 19 plate U-10Mo FEs could offer desirable improvements for cold neutron science: (a) increasing the reactor power to 30 MW provides 50% more neutron flux for cold neutron instruments, if allowed by fuel qualification and engineering constraints that have not been explored, or (b) extending the reactor cycle to 45 d offers more operating time. Thus, the ability to load more fuel in the NBSR-2 design with U-10Mo allows more flexibility in the reactor design than other LEU fuels and could lead to other optimizations that maximize cold neutron production for scientific research at the NCNR.

References

Brown N., Cuadra, A., 2015. Conversion Preliminary Safety Analysis Report for the NIST Research Reactor," No. BNL-107265-2015-IR, Brookhaven National Laboratory.
Hanson, A., Diamond, D., 2011. A Neutronics Methodology for the NIST Research Reactor Based on MCNPX, No. BNL–95208-2011-CP, Brookhaven National Laboratory.
Hanson, A., Diamond, D., 2014. Calculation of Design Parameters for an Equilibrium LEU Core in the NBSR using a U-7Mo Dispersion Fuel, No. BNL-105311-2014-IR, Brookhaven National Laboratory.
Kopetka, P., Williams, R.E., Rowe, J.M., 2006. NIST Liquid Hydrogen Cold Source, NISTIR 7352, US Department of Commerce, National Institute of Standards and Technology.
Leenaers, A. et al., 2004. Post-irradiation examination of uranium – 7 wt% molybdenum atomized dispersion fuel. J. Nucl. Mater. 335, 39–47.
Leenaers, A. et al., 2011. Irradiation behavior of ground U (Mo) fuel with and without Si added to the matrix. J. Nucl. Mater. 412, 41–52.

NIST, 2010, Safety Analysis Report (SAR) for License Renewal of the National Institute of Standards and Technology Reactor–NBSR; NBSR-14, Rev. 4. National Institute of Standards and Technology.
Pelowitz, D.B. (Ed.), 2012. MCNP6™ User's Manual, LACP-11-01708, Los Alamos National Laboratory.
Robinson, A.B., Chang, G.S., Keiser, D.D., 2009. Irradiation Performance of U-Mo Alloy Based "Monolithic" Plate-Type Fuel – Design Selection.
Ryu, H.J. et al., 2013. Post-irradiation analyses of U-Mo dispersion fuel rods of KOMO Tests. Nucl. Eng. Technol. 45, 847–858.
Snelgrove, J.L., Hofman, G.L., Meyer, M.K., Trybus, C.L., Wiencek, T.C., 1997. Development of very-high-density low-enriched-uranium fuels. Nucl. Eng. Des. 178, 119–126.
Soo, Y., Hofman, G.L., Cheon, J.S., 2013. Recrystallization and fission-gas-bubble swelling of U – Mo fuel. J. Nucl. Mater. 436, 14–22.
Turkoglu, D.J., Wu, Z., Williams, R.E., Newton, T.H., 2018. Comparison of Neutronics Performance Characteristics of the Proposed NIST Reactor With Different LEU Fuels. In: PHYSOR 2018 – Reactor Physics Paving the Way Towards More Efficient Systems, Cancun, Mexico, April 22–26.
U.S. Nuclear Regulatory Commission, 1988. Safety Evaluation Report related to the Evaluation of Uranium Silicide-Aluminum Dispersion Fuel for Use in Non-Power Reactors.
Woolstenhulme, N.E., Cole, J.I., Glagolenko, I., et al., 2016. Irradiation Tests Supporting LEU Conversion of Very High Power Research Reactors in the US, No. INL/CON-16-39776, Idaho National Laboratory, Idaho Falls, ID (United States).
Wu, Z., Williams, R.E., 2016. Core design studies on a low-enriched uranium reactor for cold neutron sources at NIST. In: PHYSOR 2016, Sun Valley, ID, May1-5, 1583–1592.
Wu, Z., Carlson, M., Williams, R.E., Rowe, J.M., 2015. A novel compact core design for beam tube research reactors. Trans. Am. Nucl. Soc. 112, 8–11.
Wu, Z., Williams, R.E., Rowe, J.M., Newton, T.H., O'Kelly, S., et al., 2017. Neutronics and safety studies on a research reactor concept for an advanced neutron source. Nucl. Technol. 199, 67–82.